Laser-induced multiphoton dissociation of H$_2^+$ as a function of the field frequency using parametric equations of motion

Dhrubajyoti Kalita and Ashish K. Gupta[*]

Department of Chemistry, Indian Institute of Technology, Guwahati 781039, Assam, India

We have applied parametric equations of motion (PEM) to study photodissociation dynamics of H$_2^+$. This is an application of PEM having frequency as the parameter to a non-Hermitian Hamiltonian. The resonances are extracted using the smooth exterior scaling method. Here we have studied how different resonance states behave with respect to the change in frequency of the laser field. The advantage of this method is that one can easily trace different resonance states that are changing as the parameter changes. It is observed that some higher lying vibrational states remain bound states in continuum with the decrease in frequency.

PACS number(s): 33.80.Rv

I. INTRODUCTION

Rabitz and co-workers [1] had put forward a method in which the Schrödinger equation was solved explicitly only once and the solutions at other parameter values were obtained by integrating a set of ordinary differential equations through the parameter space of the Hamiltonian. These equations have been termed as parametric equations of motion (PEM). These kinds of equations have been applied initially in the field of quantum chaos [2–4]. Rabitz and co-workers [1] applied PEM to several simple, illustrative examples. Later PEM was implemented by Gross *et al.* [5,6] to obtain the three-dimensional (3D) plots of population dynamics as a function of frequency and phase or amplitude. In their method, the time-dependent Schrödinger equation (TDSE) was needed to be solved once to obtain the quantum dynamic behavior in the presence of strong (nonperturbative) periodic fields having the form $A\cos(\omega t)$ over a range of field amplitudes and frequencies. This method utilizes Floquet theory as well and integrates through frequency and amplitude space using PEM for quasienergies and Floquet eigenvectors. The advantage of PEM lies in the fact that one can trace individual eigenstates in parameter space. In this paper, we have implemented PEM jointly with the smooth exterior scaling method (SES) to study the photodissociation dynamics of H$_2^+$. In this paper we are trying to accumulate information about the photodissociation dynamics of H$_2^+$ by applying PEM having field frequency as the parameter. In one of our recent publications, we have studied the photodissociation dynamics of H$_2^+$ by applying PEM having field amplitude as the parameter [7].

Intense ultrashort laser pulses are used to initiate and control molecular dynamics and have many applications in molecular science. It has been reported earlier that the H$_2$ and H$_2^+$ are the ideal systems for a detailed understanding of the ionization and dissociation dynamics of small molecules. Multiphoton dissociation (MPD) of H$_2^+$ has been studied extensively [8–12]. Many interesting phenomena viz. "bond-hardening" and "bond-softening" have been put forward. The smooth exterior scaling (SES) method is one of the known methods to generate the wave functions without any artificial reflections

occurring at the grid [13–20]. Furthermore it doesn't disturb the interaction region. In this method, one can keep as large a grid as desired without being disturbed by complex scaling. The wave functions calculated by this method can provide indisputable proof for different mechanisms. The dissociating channels can be recognized directly from the resonance wave functions. A resonance state is a long-lived state that has sufficient energy to break up into two or more subsystems. Continuum tails are part of the wave functions that are at large distances but still in the undisturbed region (due to the scaling). The SES method has been explained in detail in our three recent publications [7,19,20] as well as numerous other publications [13,14,17,21–23]. For the sake of completeness, we have discussed Floquet formalism and SES methods in Sec. II and parametric equations of motion formalism in Sec. III. Results and discussion and the conclusion drawn from this work are discussed in Secs. IV and V, respectively.

II. FLOQUET FORMALISM

Chu and co-workers [11] had calculated the complex quasienergies by diagonalizing the complex scaled Floquet Hamiltonian whose size in the Fourier grid basis depends upon the number of grid points (N), the number of electronic surfaces involved in photodissociation (m), and the number of photons absorbed (n). The dimension of the Hamiltonian matrix should be ($mN \times mN$) for a single photon excitation. The form of the Floquet Hamiltonian ($\hat{H}_f$) derived by Chu and co-workers [11] including the SES absorbing term [i.e., complex absorbing potential (V_{CAP}) term] [17,19,20] is given by

$$(\hat{H}_f)_{\alpha n,\beta m} = \left[\frac{\hat{P}^2}{2M} + U_{\alpha,\beta}(F(R)) + n\hbar\omega + \hat{V}_{\text{CAP}}\right]\delta_{\alpha\beta}\delta_{nm}$$
$$+ \left[\frac{1}{2}\vec{\mu}_{\alpha\beta}(F(R))\cdot\vec{A}_0\right]\delta_{(n,m=n\pm1)}(1-\delta_{\alpha\beta}),$$
$$(1)$$

where R is the nuclear separation and α and β denote the electronic states and indices m and n go over the Fourier expansion of the Floquet vector ranging from $+\infty$ to $-\infty$. Here μ is the dipole operator, and A_0 and ω are the amplitude and frequency of the laser, respectively. Here $F(R)$ is the path

___

[*]gupta@iitg.ernet.in

in the complex coordinate plane defined as [14]

$$\frac{\partial F}{\partial R} = 1 + [\exp(i\theta_0) - 1]g(R),$$

where $g(R)$ is varied from 0 to 1 smoothly around the point $R = R_0$ and θ_0 and λ are the scaling parameters. We have used the modified smooth exterior scaling (MSES) path [7,20]:

$$F(R) = \text{Re}^{i\theta(R)}, \tag{2}$$

where

$$\theta(R) = \{1 + 0.5\{\tanh[\lambda(R - R_0)] - \tanh[\lambda(R + R_0)]\}\}\theta_0. \tag{3}$$

Only two electronic states of H_2^+ [i.e., the ground $(1s\sigma_g)$ and the first excited repulsive $(2p\sigma_u)$ states] are considered [11].

The block structure of the Floquet Hamiltonian $[(\hat{H}_f)_{\alpha n, \beta m}]$ is given as [11]

$$H^F = \begin{pmatrix} \ddots & & & & & \\ & A + 4\omega I & B & 0 & 0 & 0 \\ & B^T & A + 2\omega I & B & 0 & 0 \\ & 0 & B^T & A & B & 0 \\ & 0 & 0 & B^T & A - 2\omega I & B \\ & 0 & 0 & 0 & B^T & A - 4\omega I \\ & & & & & \ddots \end{pmatrix},$$

where

$$A = \begin{pmatrix} T_R + U_1(F(R)) + \hat{V}_{\text{CAP}} & \frac{1}{2}\vec{\mu}_{12}(F(R)) \cdot \vec{A}_0 \\ \frac{1}{2}\vec{\mu}_{21}(F(R)) \cdot \vec{A}_0 & T_R + U_2(F(R)) + \hat{V}_{\text{CAP}} - \omega I \end{pmatrix},$$

and

$$B = \begin{pmatrix} 0 & 0 \\ \frac{1}{2}\vec{\mu}_{12}(F(R)) \cdot \vec{A}_0 & 0 \end{pmatrix}.$$

Here T_R stands for the kinetic energy operator. To put the matrices into a suitable form to apply frequency PEM, A is transformed as $A = C + D\omega$, where

$$C = \begin{pmatrix} T_R + U_1(F(R)) + \hat{V}_{\text{CAP}} & \vec{\mu}_{12}(F(R)) \cdot \vec{A}_0 \\ \vec{\mu}_{12}(F(R)) \cdot \vec{A}_0 & T_R + U_2(F(R)) + \hat{V}_{\text{CAP}} \end{pmatrix},$$

and

$$D = \begin{pmatrix} 0 & 0 \\ 0 & -I \end{pmatrix}.$$

Here we define a matrix H_0^F and P as follows:

$$H_0^F = \begin{pmatrix} \ddots & & & & & \\ & C & B & 0 & 0 & 0 \\ & B^T & C & B & 0 & 0 \\ & 0 & B^T & C & B & 0 \\ & 0 & 0 & B^T & C & B \\ & 0 & 0 & 0 & B^T & C \\ & & & & & \ddots \end{pmatrix},$$

$$P = \begin{pmatrix} \ddots & & & & & \\ & 4I + D & 0 & 0 & 0 & 0 \\ & 0 & 2I + D & 0 & 0 & 0 \\ & 0 & 0 & D & 0 & 0 \\ & 0 & 0 & 0 & -2I + D & 0 \\ & 0 & 0 & 0 & 0 & -4I + D \\ & & & & & \ddots \end{pmatrix}.$$

Now H^F can be written as

$$H^F = H_0^F + P\omega.$$

Diagonalization of the complex general matrix H^F will give the necessary quasienergies (ϵ) and the eigenvectors ψ_L and ψ_R at the initial laser field frequency (ω). H^F depends linearly on ω. More importantly these equations are in a suitable form to apply the PEM with respect to the ω as described in the next section.

III. PARAMETRIC EQUATIONS OF MOTION FORMULATION

Consider an eigenvalue problem:

$$\bar{\bar{H}}\, \bar{C}_i^{\,R} = \bar{C}_i^{\,R} E_i,$$

$$\left(\bar{C}_i^{\,L}\right)^T \bar{\bar{H}} = E_i \left(\bar{C}_i^{\,L}\right)^T,$$

where $\bar{\bar{H}}$ depends linearly on λ as

$$\bar{\bar{H}} = \bar{\bar{H}}_0 + \lambda \bar{\bar{V}},$$

where $\bar{\bar{H}}_0$ and $\bar{\bar{V}}$ are λ independent matrices and $\bar{C}_i^{\,R}$, $\bar{C}_i^{\,L}$ are the respective right and left eigenvectors of the complex general matrix $\bar{\bar{H}}$ having complex eigenvalues E_i. Superscript T stands for transpose. $\bar{C}_i^{\,R}$ and $\bar{C}_i^{\,L}$ follows the relationship,

$$\left(\bar{C}_i^{\,L}\right)^T \bar{C}_i^{\,R} = 1.$$

Following the derivation of Rabitz and co-workers [1] evolution of eigenvalues (E) and eigenvectors (C) as a function of the linear perturbation parameter λ is given as

$$\frac{\partial E_n}{\partial \lambda} = V_{nn}, \tag{4}$$

$$\frac{\partial C_i^R}{\partial \lambda} = -\sum_{j \neq i} \frac{C_j^R V_{ji}}{E_j - E_i}, \tag{5}$$

$$\frac{\partial C_i^L}{\partial \lambda} = -\sum_{j \neq i} \frac{C_j^L V_{ij}}{E_j - E_i}, \tag{6}$$

$$\frac{\partial V_{nn}}{\partial \lambda} = 2\sum_{m \neq n} \frac{V_{nm} V_{mn}}{E_n - E_m}, \tag{7}$$

$$\frac{\partial V_{mn}}{\partial \lambda} = \sum_{l \neq m,n} V_{ml} V_{ln} \left(\frac{1}{E_n - E_l} + \frac{1}{E_m - E_l} \right) + \frac{V_{mn} V_{mm}}{E_n - E_m} + \frac{V_{mn} V_{nn}}{E_m - E_n}. \tag{8}$$

Equations (4)–(8) are collectively called PEM. For the application of PEM to the photodissociation of H_2^+, V_{mn} is defined as

$$V_{mn} = \left[C_m^L(\omega) \right]^T P C_n^R(\omega). \tag{9}$$

IV. RESULTS AND DISCUSSION

We have considered the H_2^+ molecule as a test case for the PEM implementation. Here we have chosen frequency as the parameter. The necessary potential energy surface and dipole matrix are given by Chu and co-workers [11]. We have used the length gauge [11]. The Floquet electronic-field potential curve crossings are shown in Fig. 1.

Here, each Floquet channel $|g,n\rangle$ and $|e,n\rangle$ represents ground electronic ($1s\sigma_g$) and first excited electronic state ($2p\sigma_u$) potential surface, respectively, dressed by "n" photons. $|g,0\rangle$ and $|e,-1\rangle$ form a single Floquet block. In Fig. 1, potential corresponding to three Floquet blocks are shown (i.e., one Floquet block moved by 2ω is added to either side of $|g,0\rangle$ and $|e,-1\rangle$ block [11]). Here, Figs. 1(a)–1(c) describe the dressed potential at $\omega = 0.1716$, 0.1306, and 0.0865 a.u., respectively. The ground electronic ($1s\sigma_g$) state is represented by triangles whereas the first excited electronic state ($2p\sigma_u$) is represented by squares. The resulting Hamiltonian is constructed in the Fourier grid method [24]. PEM are integrated numerically using a fifth-order Runge-Kutta integrator. Before integrating the PEM through frequency space, it is important to determine the appropriate initial conditions [i.e., the quasienergies (ϵ), V_{ij} matrix elements, and eigenvectors (C_i^R and C_i^L)] at some chosen field amplitude (A_0) and initial frequency (ω). We have determined this initial condition by diagonalizing the H^F matrix [19,20]. Kinetic energy operator and SES terms are calculated as shown by Karlsson [17]. The resonances are calculated by diagonalizing this Hamiltonian. A LAPACK subroutine for
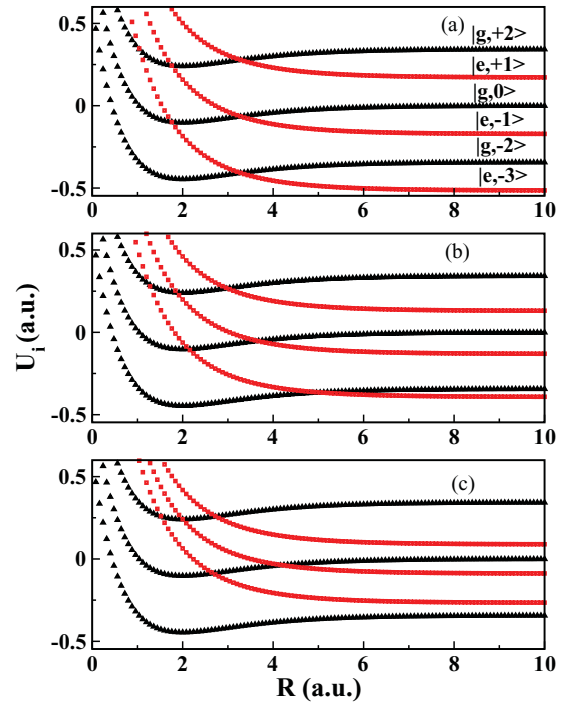

FIG. 1. (Color online) Potential-energy curves for the two electronic states of H_2^+ dressed by $n = 0, -1, -2, -3$ photons at laser field frequency (ω) = 0.1716, 0.1306, and 0.0865 a.u. are shown in (a), (b), and (c), respectively. As the frequency decreases, the crossing points move upward and toward right.
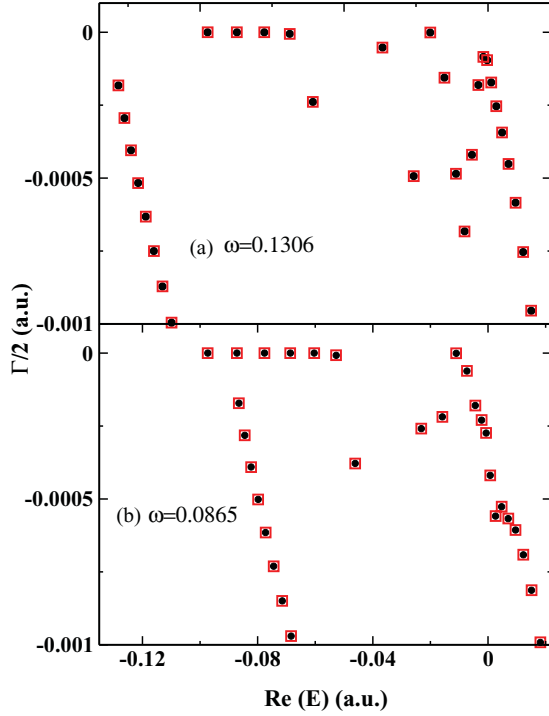
FIG. 2. (Color online) Plot of results obtained from diagonalizing the SES Hamiltonian and from solving the PEM at $\omega = 0.1306$ and 0.0865 a.u. for $A_0 = 0.005$ a.u.

general complex matrix diagonalization is used. The real part (E_r) of the eigenvalue provides the position of the resonances and the reciprocal of its imaginary part (Γ) is proportional to the lifetime of the resonances. We have used 151 basis functions. After diagonalization of the SES Hamiltonian [Eq. (1)] ϵ, C_i^R, and C_i^L are immediately obtained. Using Eq. (9) the matrix elements are obtained. The PEM are then integrated as a function of field frequency starting from 0.1716 to 0.0865 a.u. Use of the PEM is advantageous as it enables us to trace different resonance states as a function of the laser

TABLE I. Resonances for the H_2^+ molecule at the frequency 0.1306 a.u. (A) Diagonalization results. (B) PEM results.

	Real part	Imaginary part
A	−0.0973 6058 3284	−0.0000 0000 0124
B	−0.0973 6085 3284	−0.0000 0000 0124
A	−0.0872 3010 1465	−0.0000 0000 0021
B	−0.0872 3010 1465	−0.0000 0000 0021
A	−0.0770 4912 5060	−0.0000 0002 4716
B	−0.0770 4912 5060	−0.0000 0002 4716
A	−0.0688 4738 9808	−0.0000 0563 8548
B	−0.0688 4738 9808	−0.0000 0563 8548
A	−0.0608 3954 9752	−0.0002 3873 4335
B	−0.0608 3954 9752	−0.0002 3873 4335
A	−0.0534 3810 7239	−0.0012 6865 5756
B	−0.0534 3810 7239	−0.0012 6865 5756
A	−0.0439 1841 2102	−0.0017 9323 6746
B	−0.0439 1841 2102	−0.0017 9323 6746

TABLE II. Resonances for the H_2^+ molecule at the frequency 0.0865 a.u. (A) Diagonalization results. (B) PEM results.

	Real part	Imaginary part
A	−0.0973 4896 8503	−0.0000 0000 0075
B	−0.0973 4896 8503	−0.0000 0000 0075
A	−0.0872 0435 2170	−0.0000 0000 1086
B	−0.0872 0435 2170	−0.0000 0000 1086
A	−0.0776 4570 3774	−0.0000 0000 1697
B	−0.0776 4570 3774	−0.0000 0000 1697
A	−0.0686 8687 3360	−0.0000 0000 0093
B	−0.0686 8687 3360	−0.0000 0000 0093
A	−0.0603 5896 7212	−0.0000 0001 4843
B	−0.0603 5896 7212	−0.0000 0001 4843
A	−0.0527 6432 9783	−0.0000 0717 2492
B	−0.0527 6432 9783	−0.0000 0717 2492
A	−0.0461 2317 1534	−0.0003 7849 3058
B	−0.0461 2317 1534	−0.0003 7849 3058

field frequency. Otherwise, in the diagonalization method, the eigenvalues are rearranged every time and that information gets lost.

In Fig. 2, we have compared the results obtained from diagonalizing the SES Hamiltonian and from solving the PEM at two frequencies (i.e., for $\omega = 0.1306$ and 0.0865 a.u., respectively) at a fixed field amplitude $A_0 = 0.005$ a.u. Here, Fig. 1(a) shows both the SES and PEM results at $\omega = 0.1306$ a.u. The PEM results and the SES results are denoted
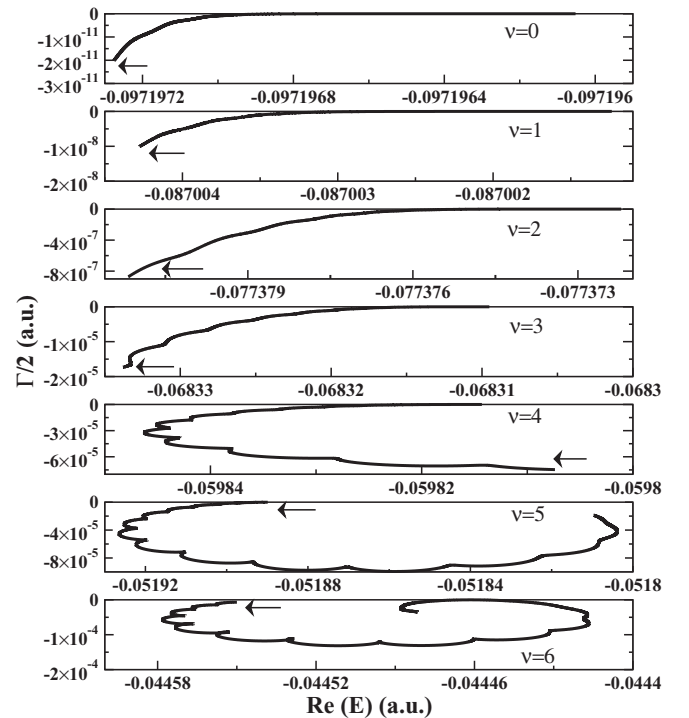

FIG. 3. Plot of the positions of resonances [i.e., real part of the quasienergies (Re (E))] versus width of resonances ($\Gamma/2$) as frequency changes from 0.1716 to 0.0865 a.u. at $A_0 = 0.001$ a.u. The starting point ($\omega = 0.1716$ a.u.) of integration is pointed by an arrow.

by open squares and solid circles, respectively. From this plot it is clear that the results obtained from PEM integration are in good concordance with the direct diagonalization results. Similarly, Fig. 1(b) shows both the SES and PEM results at $\omega = 0.0865$ a.u. This plot also shows precise agreement of results.

A better comparison of resonances obtained from the diagonalization method and the PEM at frequencies 0.1306 and 0.0865 a.u., respectively, is provided in Tables I and II, respectively. The resonances are calculated by using $\theta_0 = 0.09$ in both cases. From these tables it is clear that the results obtained from PEM integration are in good concordance with the direct diagonalization results.

In Fig. 3, we have plotted the positions [i.e., the real part of the quasienergies [Re (E)]] versus width ($\Gamma/2$) of the first seven resonances for a range of frequencies (i.e., ω goes over 0.1716–0.0865 a.u.) at $A_0 = 0.001$ a.u. Here, we have plotted $\nu = 0, 1, 2\text{–}6^{\text{th}}$ vibrational states of H_2^+ as a function of ω. The starting point of integration is pointed by an arrow. The crossing between $|g,0\rangle$ and $|e,-1\rangle$ Floquet channels (referred to as the crossing point) at $\omega = 0.1716$ a.u occurs at value -0.06624 a.u. Initially (i.e., at $\omega = 0.1716$ a.u.) the first field free state ($\nu = 0$) having position -0.09719 a.u. lies below the crossing point and therefore it obviously behaves as a bound state. As the frequency decreases further, the crossing point shifts upward and as a result the lifetime (i.e., inverse of Γ value) of this resonance state increases. The same trend is also

followed by field free states corresponding to $\nu = 1, 2$, and 3 which has positions -0.0869, -0.0774, and -0.0683 a.u., respectively. However, field free state corresponding to $\nu = 4$ having position -0.0598 a.u. initially lies at the crossing point. With the decrease in frequency, the crossing point shifts upward and as a result, this state ($\nu = 4$) lies below the crossing point. Hence, the lifetime of this state also increases with the decrease in laser frequency. On the other hand, field free states corresponding to $\nu = 5$ and 6 having positions -0.05185 and -0.04448 a.u., respectively, lie initially above the crossing point. With the decrease in frequency, these states gradually come close to the crossing point and finally lie below it. That is why the lifetime of these two states first decreases and then increases. Like Fig. 3, the positions [i.e., the real part of the quasienergies [Re (E)]] versus width ($\Gamma/2$) of the first seven resonances for a range of frequencies (i.e., ω goes over 0.1716–0.0865 a.u.) at $A_0 = 0.02$ a.u. have been plotted in Fig. 4. At this laser field amplitude (A_0) a deeper understanding of the trend followed by different resonance states as a function of field frequency (ω) is beyond the scope of the present study. Vibrationally trapped states start appearing at this amplitude [10,19]. In the case of resonance state corresponding to $\nu = 6$, it is expected that with the decrease in frequency, the lifetime (inverse of Γ) should increase due to the upward shift of the crossing point. This in turn should make other higher lying states in continuum go below the crossing point—with a subsequent increase in their lifetimes. Interestingly, from
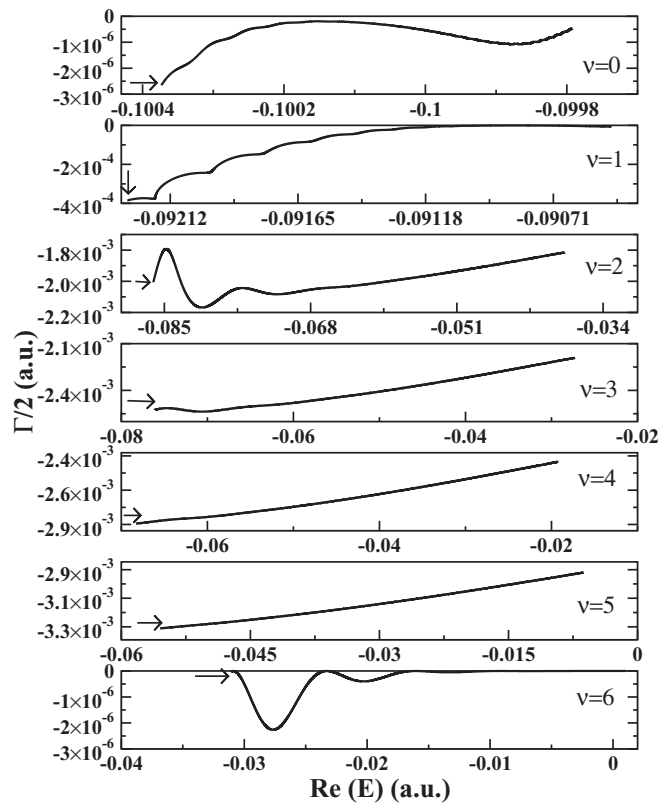

FIG. 4. Plot of the positions of resonances [i.e., real part of the quasienergies (Re (E))] versus width of resonances ($\Gamma/2$) as frequency changes from 0.1716 to 0.0865 a.u. at $A_0 = 0.02$ a.u. The starting point ($\omega = 0.1716$ a.u.) of integration is pointed by an arrow.
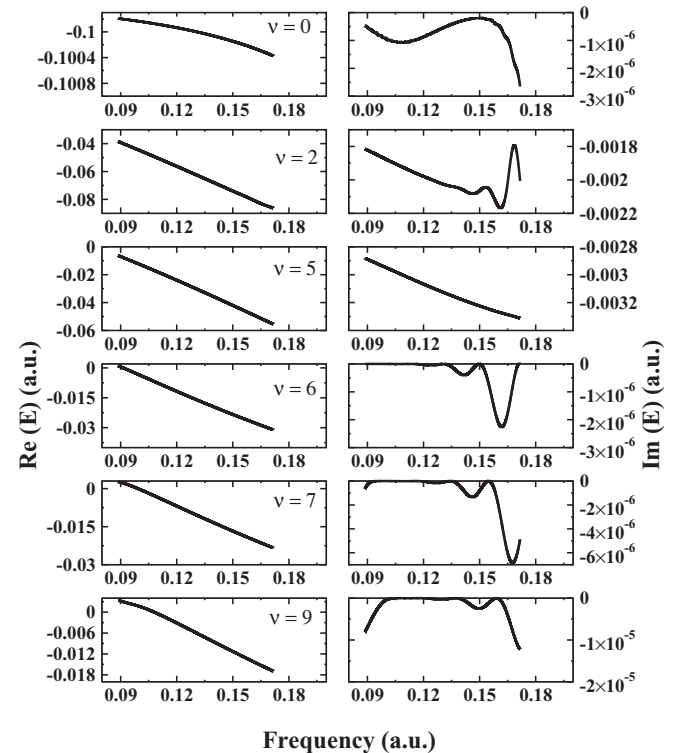

FIG. 5. Plot of the positions of resonances [i.e., real part of the quasienergies [Re (E)]] (in the left column) and width ($\Gamma/2$) (in the right column) of some bound resonances (i.e., corresponding to $\nu = 0, 2, 5, 6, 7$, and 9) versus frequency (ranging from 0.1716 to 0.0865 a.u.) at $A_0 = 0.02$ a.u.
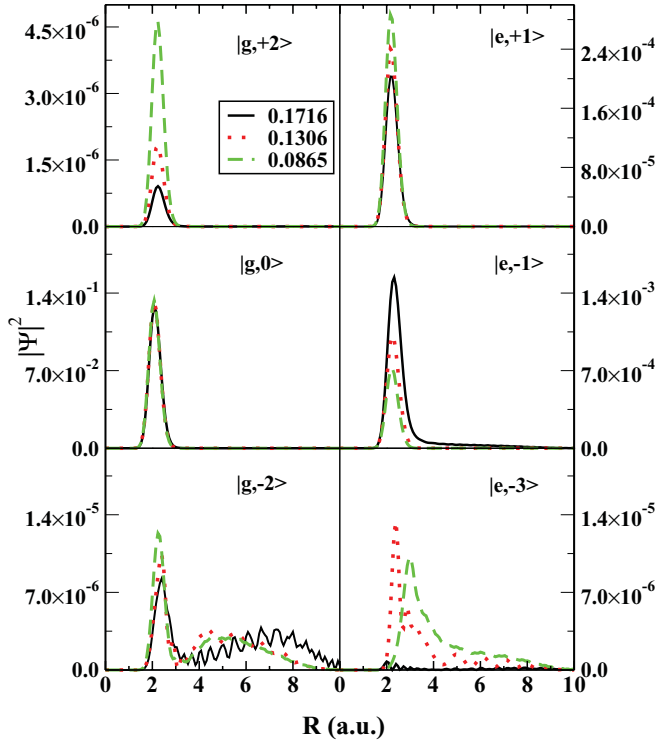
FIG. 6. (Color online) Plot of the wave function (Ψ) of the first resonance state ($\nu = 0$) corresponding to different Floquet channels for laser field frequency 0.1716 (solid line), 0.1306 (dotted line), and 0.0865 a.u. (dashed line).

FIG. 7. (Color online) Plot of the wave function (Ψ) of the seventh resonance state ($\nu = 6$) corresponding to $|g,0\rangle$, $|e,-1\rangle$ Floquet channels for laser field frequency 0.1716 (solid line), 0.1306 (dotted line), and 0.0865 a.u. (dashed line).

our calculations we see that with a decrease in frequency, the lifetime of the sixth resonance state is imperceptibly small (on the order of 10^{-6}) throughout the entire frequency domain. Hence, the state remains as the vibrationally trapped state. This state is localized over the crossing point and follows the shift of the crossing point (see Fig. 7). We have plotted the variation of Re (E) and width ($\Gamma/2$) of some bound resonances (i.e., corresponding to $\nu = 0, 2, 5, 6, 7,$ and 9) versus frequency at an amplitude (A_0) = 0.02 a.u. in Fig. 5. Here in the left column Re (E) is varied whereas in the right column width is varied as a function of laser frequency. Like Fig. 4, the same information can be obtained from this plot.

In Fig. 6, the wave function of the first resonance state ($\nu = 0$) corresponding to $|g,0\rangle$, $|e,-1\rangle$, $|g,-2\rangle$, and $|e,-3\rangle$, $|e,+1\rangle$, and $|g,+2\rangle$ Floquet channels have been plotted for three different frequencies [i.e., $\omega = 0.1716$ (solid line), 0.1306 (dotted line), and 0.0865 a.u. (dashed line)] at $A_0 = 0.02$ a.u. From this figure it has been observed that with the decrease in frequency the dissociation of the state increases. This increase in dissociation is mainly due to an increase in dissociation via the $|e,-3\rangle$ Floquet channel. Hence we can conclude that the photodissociation of H_2^+ by three-photon absorption becomes dominant at lower frequency. In Fig. 7, the wave function of the seventh resonance state ($\nu = 6$) corresponding to the $|g,0\rangle$ and $|e,-1\rangle$ Floquet channels for frequencies $\omega = 0.1716$ (solid line), 0.1306 (dotted line), and 0.0865 a.u. (dashed line) at $A_0 = 0.02$ a.u. have been plotted. From this figure it is clear that with the decrease in frequency the center of this state gets shifted and coincides with
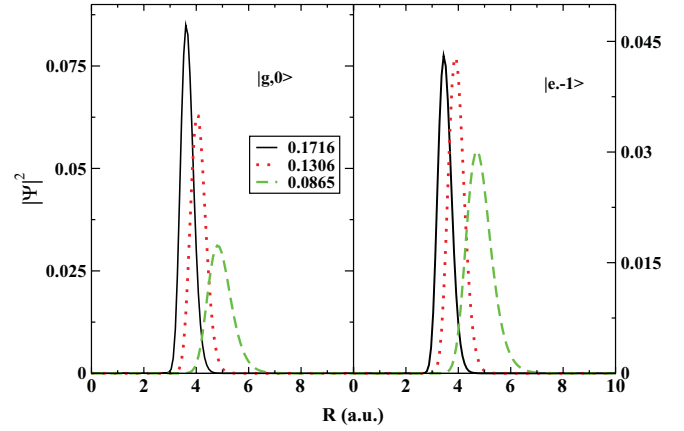
the crossing point. As the frequency decreases the crossing between states (i.e., $|g,0\rangle$ and $|e,-1\rangle$) will occur at higher energy and higher nuclear separation. So this vibrationally trapped state will also be centered on higher nuclear separation value. Thus this state remains the bound state in the continuum with the decrease in frequency as mentioned in Fig. 4.

Though computationally matrix diagonalization is 10 times faster than the PEM method, the efficiency of the PEM lies in the fact that the variation of a specific resonance state with respect to a range of field frequency can be easily traced which is shown in Figs. 3 and 4, respectively. This is because in PEM the line number of a particular resonance state remains fixed in output whereas in the matrix diagonalization it is rearranged every time. In one of our recent publications [7], we have described the outcome of PEM where amplitude acts as a parameter. One reason for PEM being slow is the very high accuracy demanded during the propagation of the equations as is evident from the two tables in discussion.

V. CONCLUSION

In summary, we have implemented PEM where frequency is chosen as the parameter to study the photodissociation dynamics of H_2^+. The resonance states are calculated with the help of the SES method. Here we are able to trace different vibrational states as a function of frequency. We can see very clearly that some higher lying vibrational states remain bound states in continuum with the decrease in frequency.

ACKNOWLEDGMENTS

[1] D. A. Mazziotti, M. K. Mishra, and H. A. Rabitz, J. Phys. Chem. **99**, 112 (1995).

[2] P. Pechukas, Phys. Rev. Lett. **51**, 943 (1983).

[3] T. Yukawa, Phys. Lett. A **116**, 227 (1986).

[4] X. Yang and J. Burgdorfer, Phys. Rev. A **48**, 83 (1993).

[5] A. K. Gupta, P. Gross, D. B. Bairagi, and M. K. Mishra, Chem. Phys. Lett. **257**, 658 (1996).

[6] P. Gross, A. Gupta, D. B. Bairagi, and M. K. Mishra, Chem. Phys. Lett. **236**, 8 (1995).

[7] D. J. Kalita, A. Rao, I. Rajvanshi, and A. K. Gupta, J. Chem. Phys. **134**, 224309 (2011).

[8] A. Giusti-Suzor, X. He, O. Atabek, and F. H. Mies, Phys. Rev. Lett. **64**, 515 (1990).

[9] P. H. Bucksbaum, A. Zavriyev, H. G. Muller, and D. W. Schumacher, Phys. Rev. Lett. **64**, 1883 (1990).

[10] A. Giusti-Suzor and F. H. Mies, Phys. Rev. Lett. **68**, 3869 (1992).

[11] S.-I. Chu, J. Chem. Phys. **94**, 7901 (1991).

[12] K. Sandig, H. Figger, and T. W. Hansch, Phys. Rev. Lett. **85**, 4876 (2000).

[13] N. Moiseyev, J. Phys. B **31**, 1431 (1998).

[14] N. Rom, E. Engdahl, and N. Moiseyev, J. Chem. Phys. **93**, 3413 (1990).

[15] H. O. Karlsson, J. Chem. Phys. **108**, 3849 (1998).

[16] N. Elander and E. Yarevsky, Phys. Rev. A **57**, 3119 (1998).

[17] H. O. Karlsson, J. Chem. Phys. **109**, 9366 (1998).

[18] D. A. Telnov and S.-I. Chu, Phys. Rev. A **59**, 2864 (1999).

[19] D. J. Kalita and A. K. Gupta, J. Chem. Phys. **133**, 134303 (2010).

[20] D. J. Kalita and A. K. Gupta, J. Chem. Phys. **134**, 094301 (2011).

[21] N. Moiseyev and J. O. Hirschfelder, J. Chem. Phys. **88**, 1063 (1988).

[22] T. N. Rescigno, M. Baertschy, D. Byrum, and C. W. McCurdy, Phys. Rev. A **55**, 4253 (1997).

[23] N. Moiseyev, Phys. Rep. **302**, 211 (1998).

[24] C. C. Marston and G. G. Balint-Kurti, J. Chem. Phys. **91**, 3571 (1989).